



Published in final edited form as:

Leukemia. 2024 February ; 38(2): 291–301. doi:10.1038/s41375-023-02131-4.

FLT3 tyrosine kinase inhibition modulates PRC2 and promotes differentiation in acute myeloid leukemia

Pamela J. Sung^{1,2,*}, Murugan Selvam¹, Simone S. Riedel³, Hongbo M. Xie⁴, Katie Bryant¹, Bryan Manning², Gerald B. Wertheim⁵, Katarzyna Kulej⁶, Lucie Pham¹, Robert L. Bowman⁷, Jennifer Peresie⁸, Michael J. Nemeth⁸, Ross L. Levine⁹, Benjamin A. Garcia^{6,10}, Sara E. Meyer¹¹, Simone Sidoli^{6,12}, Kathrin M. Bernt³, Martin Carroll²

¹Department of Medicine – Leukemia, Department of Pharmacology & Therapeutics, Roswell Park Comprehensive Cancer Center; Buffalo, NY, USA

²Department of Medicine, Division of Hematology/Oncology, University of Pennsylvania, Perelman School of Medicine; Philadelphia, PA, USA

³Department of Pediatrics, Children’s Hospital of Philadelphia and Department of Pediatrics, University of Pennsylvania, Perelman School of Medicine and Abramson Cancer Center; Philadelphia, PA, USA

⁴Department of Biomedical and Health Informatics, Children’s Hospital of Philadelphia; Philadelphia, PA, USA

⁵Department of Pathology, Children’s Hospital of Philadelphia; Philadelphia, PA, USA

⁶Department of Biochemistry and Biophysics, University of Pennsylvania, Perelman School of Medicine; Philadelphia, PA, USA

⁷Department of Cancer Biology, University of Pennsylvania, Perelman School of Medicine; Philadelphia, PA, USA

⁸Department of Immunology, Roswell Park Comprehensive Cancer Center; Buffalo, NY, USA

⁹Human Oncology and Pathogenesis Program, Memorial Sloan Kettering Cancer Center; New York, NY, USA

¹⁰Department of Biochemistry and Molecular Biophysics, Washington University in St. Louis; St. Louis, MO, USA

*Corresponding author: Correspondence: Pamela J. Sung, MD PhD, Pamela.Sung@roswellpark.org, Elm and Carlton St, CGP L4-318, Buffalo, NY 14263, Fax: (716) 845-8346.

Author Contributions: PJS and MC designed all experiments, interpreted all data, and wrote the manuscript. SS, KK, and BAG performed and analyzed proteomic experiments. SSR, HMX, and KMB performed and analyzed ChIP-Seq experiments. KMB provided intellectual input and experimental guidance on functional genomics. KB and BM performed trametinib experiments and assisted with animal studies. MS and LP performed experiments for revisions. GW performed pathology assessment of murine histology. RLB and RLL provided *Flt3^{ITD} Npm1^C* AML cells and experimental guidance. JP and MJN developed the spectral flow cytometry panel and assisted with analysis. SEM provided *Flt3^{ITD} Dnmt3a^{KO}* mice and experimental guidance. All authors reviewed and approved the manuscript.

Data availability statement: Mass spectrometry raw files generated in this study are publicly available in the Chorus repository (<http://www.chorusproject.org>) at the project number 1806. Analyzed data from proteome, ChIP sequencing, and RNA sequencing studies are available in the supplemental files. Raw ChIP-seq files were deposited to GEO (GSE243857).

¹¹Department of Pharmacology, Physiology, and Cancer Biology, Thomas Jefferson University, Sidney Kimmel Cancer Center; Philadelphia, PA, USA

¹²Department of Biochemistry, Albert Einstein College of Medicine; New York, NY, USA

Abstract

Internal tandem duplication mutations in *fms-like tyrosine kinase 3 (FLT3-ITD)* are recurrent in acute myeloid leukemia (AML) and increase the risk of relapse. Clinical responses to FLT3 inhibitors (FLT3i) include myeloid differentiation of the *FLT3-ITD* clone in nearly half of patients through an unknown mechanism. We identified enhancer of zeste homolog 2 (EZH2), a component of polycomb repressive complex 2 (PRC2), as a mediator of this effect using a proteomic-based screen. FLT3i downregulated EZH2 protein expression and PRC2 activity on H3K27me3. *FLT3-ITD* and loss-of-function mutations in *EZH2* are mutually exclusive in human AML. We demonstrated that FLT3i increase myeloid maturation with reduced stem/progenitor cell populations in murine *Flt3-ITD* AML. Combining EZH1/2 inhibitors with FLT3i increased terminal maturation of leukemic cells and reduced leukemic burden. Our data suggest that reduced EZH2 activity following FLT3 inhibition promotes myeloid differentiation of *FLT3-ITD* leukemic cells, providing a mechanistic explanation for the clinical observations. These results demonstrate that in addition to its known cell survival and proliferation signaling, FLT3-ITD has a second, previously undefined function to maintain a myeloid stem/progenitor cell state through modulation of PRC2 activity. Our findings support exploring EZH1/2 inhibitors as therapy for *FLT3-ITD* AML.

INTRODUCTION

Fms-like tyrosine kinase 3 (FLT3) is the most frequently mutated gene in acute myeloid leukemia (AML).¹ FLT3 is a type III receptor tyrosine kinase normally expressed in the hematopoietic system that is activated through binding of FLT3 ligand. *Flt3* is not essential for myeloid development in mice, though loss of *Flt3* impairs myeloid reconstitution in competitive transplantation models suggesting a role in stem and progenitor cell fitness.² Mutations in *FLT3* occur as two main sub-types, internal tandem duplications (ITD) and tyrosine kinase domain (TKD) mutations, both of which render FLT3 constitutively active.³ ⁴ *FLT3-ITD* mutations are the more common sub-type, occurring in ~25% of AMLs. *FLT3-ITD* mutations also confer inferior clinical outcomes related to high white blood cell counts on presentation and increased rates of relapse.⁵ Incorporation of FLT3 tyrosine kinase inhibitors (FLT3i) into initial therapy for *FLT3*-mutated AML has improved overall survival for patients with this disease, but unfortunately, relapses are still common.^{6, 7} Selective and potent FLT3i, such as quizartinib and gilteritinib, are effective as single agents in the relapsed and refractory setting but are not curative.^{8, 9} Therefore, further improvements to FLT3 targeted therapy are needed.

The functional impact of the ITD mutation was initially characterized in the cytokine-dependent 32D murine cell line.¹⁰ Subsequent studies in *FLT3-ITD* human cell lines demonstrated the dependency of these cell lines on activated FLT3 signaling for cell survival.¹¹ Based on these early studies, the clinical response to FLT3i was expected to

be primarily cytotoxic. Surprisingly, nearly half of all patients treated with quizartinib responded with evidence of differentiation of the leukemic clone.^{12, 13} This is a presumptive FLT3i class effect as similar findings were seen with gilteritinib¹⁴. Differentiation with FLT3i is incomplete as these patients all have residual *FLT3-ITD* clonal hematopoiesis. Incomplete differentiation predicts for worse overall survival compared to effective cytotoxic responses as it represents a measurable residual disease (MRD) positive state.¹⁵ Further promoting differentiation with FLT3i may be beneficial analogous to the addition of arsenic to all-*trans* retinoic acid (ATRA) in acute promyelocytic leukemia (APL), which increases differentiation and cures over 90% of patients with this AML subtype.¹⁶

The clinical evidence of FLT3i-induced differentiation suggests that a major function of FLT3-ITD is to maintain leukemic cells in a stem and progenitor cell state. Indeed, single cell RNA-sequencing and *FLT3* genotyping from a primary AML suggested enrichment of *FLT3-ITD* in cell populations with stem cell signatures.¹⁷ Both stem cell and leukemic cell maintenance have been demonstrated to require, in part, activity of the histone methyltransferase, enhancer of zeste homolog 2 (EZH2), a catalytic component of Polycomb repressive complex 2 (PRC2).^{18–22} In this study, we found that EZH2 is downregulated following inhibition of FLT3-ITD. We reasoned that FLT3i promote differentiation through downregulation of EZH2. We recapitulated FLT3i-induced differentiation in murine models of *FLT3-ITD* AML and demonstrated that the addition of complete PRC2 inhibition to FLT3i reduced leukemic burden and enhanced differentiation. Our results suggest a new approach to treatment of *FLT3-ITD* AML.

METHODS

Additional detailed methods are provided in the supplemental materials.

Animal model –

Mice were maintained at the Laboratory Animal facility at Roswell Park. All animal breeding and experiments were approved by our Institutional Animal Care and Use Committee. Primary AML splenocytes were harvested from moribund *Flt3^{ITD/ITD} Dnmt3a^{fl/fl} Mx1-Cre* mice²³ and injected into sub-lethally irradiated (500 cGy) 6-8 week old syngeneic BoyJ mice (B6.SJL-*Ptprc^a*, Jackson Labs). Sample size was limited to 5 mice per cohort based on availability of cells from the donor mouse. Peripheral blood was analyzed two weeks post-injection for engraftment (%CD45.2+). Mice were allocated to treatment cohorts to ensure equal mean levels of engraftment across cohorts. Animals were treated with vehicle (0.5% methylcellulose + 10% DMSO), valemestostat (ChemieTek) 100 mg/kg daily, gilteritinib (ChemieTek) 60 mg/kg thrice weekly, or valemestostat + gilteritinib. All treatments were given by oral gavage for 4 weeks. Mice were euthanized at the end of treatment. Spleens and bone marrow were collected for histology and flow cytometric analysis. Spleens were weighed before and after removing a portion for fixation in 4% paraformaldehyde for histology. Total CD45.2+ cell number per mouse was calculated by (cell number per mg of cut spleen after red blood cell (RBC) lysis x initial spleen weight x CD45.2+ percentage in spleen) plus (total cell number from both femurs after RBC lysis x CD45.2+ percentage in BM). Spleen tissues were stained with hematoxylin & eosin (H&E).

Bone marrow cytopspins were prepared prior to RBC lysis and stained with Wright-Giemsa. Morphologic evaluation was performed in a blinded fashion by a hematopathologist.

Flow cytometry –

Murine secondary AML cells were harvested as above. RBCs were depleted using RBC Lysis buffer (Biolegend). Cells were viably frozen prior to analysis. Thawed cells were stained with a 26-color single-tube panel (Table S1) in Brilliant Stain Buffer (BD Biosciences) with True-Stain Monocyte Blocker (Biolegend). Samples were analyzed on a Cytex Aurora spectral flow cytometer and FlowJo v10 (BD Biosciences). Gating strategy for specific cell lineages was performed as previously described.²⁴ Lineage negative (Lin-) cells defined as lacking CD3, B220, NK1.1, and Ter119 to separately analyze Ly6G. Percentages were excluded in analyses if the denominator was < 1000 cells.

Statistics –

All statistics not otherwise described in the methods or figure legends were performed using two-tailed Student t test in Prism 9 (GraphPad). Number of independent replicates used for statistical calculations are noted in the legends. Asterisks denote statistical significance versus control condition unless otherwise indicated (*-p<0.05, **-p<0.01, ***-p<0.01, ****-p<0.001). See Datafile S1 for additional details and summary of p-values.

RESULTS

Proteomic-based screen identifies FLT3-ITD regulation of EZH2

Myeloid differentiation is frequently seen as a consequence of drugs that target transcriptional or epigenetic mechanisms in AML, such as ATRA, isocitrate dehydrogenase 1/2 (IDH1/2) inhibitors, or Menin inhibitors.^{25–28} Based on the differentiation response seen in a substantial number of patients treated with FLT3i, we hypothesized that FLT3i, in addition to affecting growth and survival signaling, has direct or indirect effects on the transcriptional regulation of myeloid differentiation. To identify novel downstream targets of FLT3-ITD, we performed a proteomic-based screen in a human *FLT3-ITD* cell line, MV4;11 (Figure 1A, Datafile S2 and S3). Cells were treated over 16 hours with quizartinib, a selective second-generation FLT3 inhibitor. Samples were analyzed for both the phospho-proteome and total proteome, followed by unsupervised clustering analysis to filter for monotonic trends over time. We found that quizartinib rapidly decreased EZH2 total protein, which was associated with a transient increase in EZH2 phospho-T487 (Figures 1B,S1,S2A). This phosphorylation site has previously been characterized as downstream of CDK1 and targets EZH2 for degradation.²⁹ Indeed, we additionally found a decrease in the inhibitory phosphorylation of CDK1 at Y15 with no significant change in CDK1 total protein (Figures 1C,S2B). Decreases in total EZH2 protein and phospho-Y15 CDK1 expression over time were validated by immunoblot in MV4;11 and a second *FLT3-ITD* cell line, MOLM14 (Figures 1D–G). These changes initiate at early time points (< 6 hours) and precede major changes in cell cycle or apoptosis (Figures S2C–F), suggesting that they are not secondary to these broader cellular processes. EZH2 was not affected by FLT3i in FLT3 wild-type AML cell lines (Figure S3). CDK1 inhibition with BMS-265246 prevents FLT3i-induced EZH2 downregulation in MV4;11, yet this same effect was not

seen in MOLM14 (Figures 1H–I, S4A). Our results demonstrate that FLT3-ITD affects both EZH2 protein abundance and phosphorylation, but the mechanism of EZH2 regulation varies between cell lines.

A previous report demonstrated that loss of EZH2 protein expression in AML confers resistance to multiple therapies including FLT3i.³⁰ These data showed that long-term culture of MV4;11 cells with the multi-kinase inhibitor, midostaurin, allows for outgrowth of FLT3i resistant clones with decreased EZH2 expression. By contrast, MV4;11 cells treated with the EZH2 inhibitor, GSK126, remained sensitive to quizartinib (Figures S4B–D). Similarly, rescue of EZH2 expression by CDK1 inhibition did not enhance sensitivity to quizartinib (Figure S4D). Our data suggest that short-term EZH2 inhibition does not result in primary resistance to FLT3-selective therapy.

To determine if EZH2 is a clinically relevant target in *FLT3-ITD* AML, we assessed EZH2 expression in response to 0 to 50 nM gilteritinib, which is approximately 5-fold lower than trough concentrations for the standard dose of gilteritinib measured clinically.³¹ Total EZH2 expression decreased in a dose-dependent manner in fourteen primary *FLT3-ITD* AML samples with at least a 15% reduction in EZH2 in 2 and 9 samples for 10 nM and 50 nM gilteritinib, respectively (Figures 2A–B and S5; Table S2). Furthermore, as *EZH2* loss-of-function mutations occur in ~2% of AML, we hypothesized that if EZH2 activity contributes to FLT3-ITD leukemogenesis, these mutations would not occur in *FLT3-ITD* AML. Indeed, we found that *EZH2* and *FLT3-ITD* were mutually exclusive with a log₂ Odds ratio < -3 and p = 0.01 (Figures 2C–D).^{32–35} Overall, these results support the conclusion that EZH2 is a target of FLT3 signaling in primary human AML.

FLT3 inhibition induces EZH2 protein instability

Due to the rapidity of EZH2 reduction seen in the proteomic screen, we next assessed if FLT3i destabilizes EZH2 protein. We treated MOLM14 and MV4;11 cells with DMSO or quizartinib for 18 hours followed by a 6-hour cycloheximide treatment to inhibit new protein synthesis. Quizartinib significantly decreased EZH2 protein half-life (Figures 3A–D), demonstrating that FLT3i decrease EZH2 expression at the protein level. As EZH2 is one of several components of PRC2, we next assessed if other PRC2 proteins were similarly downregulated by FLT3i. EZH1, suppressor of zeste 12 homolog (SUZ12), and embryonic ectoderm development (EED) protein expression were stable after FLT3i treatment (Figure 3E). Since EZH2 expression levels change with cell cycle progression and FLT3i induce G1 arrest, we tested EZH2 expression levels in response to G1 arrest by serum starvation. While FLT3i in full serum (10%) reduced EZH2 expression, overnight serum deprivation (0%) had no impact (Figures 3F–G). This suggests that the downregulation of EZH2 in response to FLT3i is not secondary to FLT3i-induced cell cycle arrest.

The RAS/MAPK and PI3K/AKT pathways have previously been shown to increase EZH2 expression in lung and pancreatic cancer cell lines.^{36, 37} As both pathways are activated by FLT3-ITD, we hypothesized that MEK, AKT, or mTORC1 inhibition would reduce EZH2 expression similarly to FLT3i. Trametinib (MEK inhibitor) demonstrated a modest reduction in EZH2 expression whereas capivasertib (AKT inhibitor) and rapamycin (mTORC1 inhibitor) had lesser effects (Figures 3H–I). Cycloheximide chase with MEK inhibition

showed only a slight decrease in EZH2 protein instability, demonstrating that decreased MEK activity does not account for the full effect seen with FLT3i (Figure S6).

FLT3 inhibition functionally downregulates PRC2 activity

The primary function of EZH2 is to catalyze histone 3 lysine 27 trimethylation (H3K27me3) as part of the PRC2 complex. H3K27me3 at promoters and enhancers is associated with transcriptional silencing. We hypothesized that FLT3i promote myeloid differentiation by reducing EZH2 and, therefore, PRC2 activity. Indeed, FLT3i treatment reduced global H3K27me3 in MV4;11 and MOLM14 (Figures 4A–B). MOLM14 cells showed a ~40% reduction in H3K27me3 at 24 hours, which did not reduce further at later time points likely due to increased cell death. Maximal inhibition of H3K27me3 occurred with 7 days of FLT3i treatment in MV4;11 cells, which required supplementation with interleukin 3 (IL-3) to maintain sufficient cell survival for analysis.³⁸ To assess the impact of FLT3i on H3K27me3 at the genomic level, we performed H3K27me3 ChIP-Seq in MOLM14 cells after 24 hours of DMSO or quizartinib treatment. We chose this cell line and time point to minimize the contribution of secondary effects from differentiation and cell death and maximize the reduction in H3K27me3. At the individual peak level, 12716 peaks were unique to the DMSO condition and therefore lost upon FLT3i treatment (Figure 4C; Datafile S4). Global H3K27me3 peak distribution with respect to the transcription start site (TSS) was as expected (Figures 4D, S7A–C). We next mapped the H3K27me3 peaks across the gene body of a well-established, stem cell associated PRC2 target gene set genetically defined in murine embryonic stem (ES) cells.^{20, 39} H3K27me3 peaks enriched at the TSS of the PRC2 target module in the DMSO control condition but not in other stemness associated modules (Myc, ES cell core, and DNA binding targets) as expected (Figure 4E). The PRC2 target peaks were reduced in the quizartinib condition whereas the other modules were overall unchanged (Figure 4F). This documents the specific enrichment of H3K27me3 and its loss upon FLT3 inhibition over a set of genes associated with stemness in ES cells and cancer.

Prior RNA expression analysis of quizartinib treated cell lines have largely been conducted at early time points when apoptosis is the predominant feature or at late time points when resistance has developed.^{40, 41} To determine the impact of FLT3i-induced EZH2 downregulation on RNA expression, we compared MV4;11 cells treated with DMSO, quizartinib, or an EZH1/2 inhibitor (UNC1999) for 7 days with IL-3 to rescue cell survival from FLT3 inhibition (Figure 5A). Apoptotic cells were removed by magnetic separation. Genes downregulated with quizartinib were associated with gene ontology (GO) terms related to cell growth and proliferation as expected due to the known cell cycle arrest that occurs in these conditions (Figure S7D; Datafile S5). Genes upregulated with quizartinib were associated with GO terms related to the inflammatory response, suggestive of differentiation with increased expression of mature myeloid genes (Figure S7E). Genes with lost H3K27me3 peaks at the TSS trended towards increased RNA expression (Figure S7F). Comparison of differentially expressed genes (defined as log₂ fold change [log₂FC] 1 or -1 and adjusted p [p-adj] 0.05) for UNC1999 and quizartinib identified 253 overlapping genes (Figure 5B). To ensure that the addition of IL-3 did not substantially impact the gene targets of PRC2, we compared our UNC1999 gene expression signature

with MV4;11 cells treated with the EZH2 inhibitor GSK126 alone.⁴² As expected, genes upregulated upon EZH2 inhibition (EZH2i_UP) strongly enriched in UNC1999 (EZH1/2i) cells versus control (Figure 5C). Importantly, the GSK126 gene set was also enriched in quizartinib treated cells versus control, demonstrating that FLT3i upregulate PRC2 target genes (Figure 5D). Moreover, an ATRA-response signature obtained in APL cells was positively enriched in both UNC1999 and quizartinib treated cells consistent with myeloid differentiation (Figures 5E–F).⁴³ Prior studies have suggested a role for upregulation of the myeloid transcription factor, *CCAAT/enhancer-binding protein alpha (CEBPA)*, in FLT3i-induced differentiation.⁴⁴ *CEBPA* had a small but significant increase with both quizartinib and UNC1999 ($\log_2FC = 0.37$, $p\text{-adj} = 4.9 \times 10^{-5}$ and $\log_2FC = 0.33$, $p\text{-adj} = 7.1 \times 10^{-4}$, respectively). Altogether these data demonstrate that quizartinib functionally downregulates PRC2 activity in *FLT3-ITD* AML and increases expression of genes related to myeloid maturation.

FLT3 and PRC2 inhibition promote myeloid differentiation in vitro

While MV4;11 and MOLM14 cells are FLT3-ITD dependent, they also harbor *lysine methyltransferase 2A (KMT2A)* rearrangements, which is sufficient for leukemogenesis on its own.⁴⁵ In the presence of the strong *KMT2A* driver, treatment of these AML cell lines with FLT3i demonstrate only modest increases in myeloid differentiation markers and morphologically mature cells in the background of significant cell death.^{13, 46} FLT3i increased expression of the myeloid maturation marker, CD11b, in MV4;11 cells; however, we observed no combinatorial effect with addition of the EZH2 inhibitor, GSK126, at 7 days of treatment (Figure S8A,B). *FLT3-ITD* and *KMT2A* rearrangements infrequently co-occur in human AML.¹ Rather *FLT3-ITD* and *DNMT3A* mutations are commonly found together. Additionally, during our studies, the FLT3 inhibitor gilteritinib achieved FDA-approval for AML treatment. Thus to model FLT3i-induced differentiation in genetic and treatment settings similar to human AML, we utilized a *Flt3^{ITD} Dnmt3a^{KO}* murine AML model and gilteritinib instead of quizartinib as the FLT3i.²³ Isolated Kit⁺ AML from *Flt3^{ITD} Dnmt3a^{KO}* mice demonstrated reduced colony forming potential in the presence of gilteritinib, which was more pronounced on secondary plating (Figure 6A). Equal numbers of live cells were used for secondary plating; thus, the reduction in colonies on replating suggests a reduction in stem and progenitor cell function. Quantification of differentiated colonies by morphology on the first plating confirmed the presence of more mature myeloid cells with FLT3i treatment (Figure 6B). Treatment with UNC1999 alone modestly reduced re-plating efficiency and was associated with a small increase in morphologically differentiated colonies. Treatment with gilteritinib and UNC1999 in combination exhibited the highest reduction in colony forming activity and highest increase in differentiated colonies. These findings were validated in a cell line derived from a second murine *FLT3-ITD* AML model with the *Npm1c* co-mutation (*Flt3^{ITD} Npm1^c*).⁴⁷ Both UNC1999 and gilteritinib variably increased the percentage of mature myeloid cells (Kit⁻ CD11b⁺) whereas the combination was more consistently effective (Figures 6C–D). Knockdown of *Ezh1* or *Ezh2* in *Flt3^{ITD} Npm1^c* similarly demonstrated increased maturation that was more pronounced in combination with FLT3i (Figure S8C).

To determine if the combination of FLT3 and PRC2 inhibitors could be clinically translated, we performed colony assays in six *FLT3-ITD* patient AML bone marrow mononuclear cells (BM MNCs) with the EZH2 inhibitor, tazemetostat, or the EZH1/2 inhibitor, valemestostat (Figure 6E and S8D–E; Table S1). Tazemetostat is FDA-approved for follicular lymphoma and epithelioid sarcoma.⁴⁸ Valemestostat is currently under Phase II clinical investigation with promising results in adult T-cell leukemia/lymphoma leading to its approval in Japan.⁴⁹ Consistent with our prior study, all six samples were largely resistant to gilteritinib monotherapy despite their high *FLT3-ITD* allelic ratio.³⁸ Tazemetostat alone had similar efficacy to gilteritinib and had a varied impact in combination with gilteritinib. Valemestostat alone was highly effective in all but two samples (samples 16-0760 and 1932). All six samples were markedly sensitive to the gilteritinib and valemestostat combination. Interestingly, sample 16-0760 was resistant to gilteritinib alone and valemestostat alone but was still sensitive to the gilteritinib and valemestostat combination, demonstrating synergistic activity. The efficacy of valemestostat alone was leukemia-specific as granulocyte-monocyte colonies (CFU-GM) from normal human BM MNCs increased with treatment, consistent with a prior report of increased stem cell cycling (Figure 6F).⁵⁰ This increase in CFU-GM was not evident with the combination treatment. Although burst forming erythroid (BFU-E) colonies were notably absent with valemestostat, valemestostat did not show a major clinical effect on red blood cells beyond what was expected for patients with hematologic malignancies. These data suggest a potential role for residual PRC2 activity with FLT3i in maintaining leukemia stem and progenitor cell function from incomplete EZH2 inhibition and/or compensatory EZH1 activity, both of which can be therapeutically targeted.

Combined FLT3 and PRC2 inhibition reduces leukemic burden in vivo

We next assessed the efficacy of gilteritinib and valemestostat on *FLT3-ITD* AML in vivo using the *Flt3^{ITD} Dnmt3a^{KO}* model (Figure 7A). Whole leukemic splenocytes from moribund primary *Flt3^{ITD} Dnmt3a^{KO}* AML mice were transplanted into sub-lethally irradiated healthy syngeneic mice. After confirmation of engraftment (Figure S9A), mice were treated with vehicle, valemestostat, gilteritinib, or the combination for 4 weeks. No toxicity was seen over the course of treatment (Figure S9B). All mice were analyzed at the end of treatment for leukemic burden. Histologic sections of spleen and cytopins of bone marrow in the vehicle treated mice demonstrated marked red pulp expansion in the spleen and a predominance of blasts in the marrow, consistent with AML (Figures 7B–C). Samples from mice treated with valemestostat alone continued to show red pulp expansion and marrow blasts. Gilteritinib treated samples showed myeloid maturation in both the red pulp and the marrow, consistent with residual myeloproliferation. Strikingly, the combination treated mice showed abundant neutrophils with virtually no leukemic blasts in the marrow and a marked reduction in splenic red pulp. Spleen weight and total leukemic burden (CD45.2+ cells) were significantly reduced with all drug treatments but most substantially with the combination (Figures 7D–E, S9C). Notably, a high percentage of CD45.2+ cells remained in both spleen and bone marrow of combination treated mice, indicative of differentiation of the leukemic clone given the histologic findings (Figures S9D–E). Further characterization of the CD45.2+ cells (Figure S10) demonstrated a significant reduction in leukemic stem cells (Lin-Sca1+ Kit+, LSK) and leukemic progenitor cells (Lin-Sca1-Kit+, LS-K+) with the combination treatment in both spleen (Figures 7F–G) and bone marrow

(Figures S9F–G). This was associated with an increase in more mature donor-derived hematopoietic cells including Kit⁺ CD11b⁺ myeloid progenitors, neutrophils (Lin-Kit-CD11b⁺ SiglecF-Ly6G⁺), and megakaryocyte/erythroid progenitors (PreMegE, Lin-Sca1-Kit⁺ CD41-CD16/32^{lo} CD150⁺) (Figures 7H–I, S9H–J).⁵¹ Surprisingly, we additionally identified an expansion of splenic B- and T-lymphocytes in both gilteritinib treated groups, potentially representing non-myeloid differentiation of the leukemic clone (Figure S9K–L). Overall, we have effectively modeled the clinical finding of FLT3i-induced differentiation in vivo and demonstrated that the addition of PRC2 inhibition is an effective therapeutic strategy to further promote terminal maturation of the leukemic clone.

DISCUSSION

Significant progress has been made in the treatment of *FLT3-ITD* AML in the last decade. However, the precise mechanisms of FLT3-ITD transformation and obtaining consistent sustained clinical responses with FLT3 inhibition remain elusive. In this study, we found that FLT3 inhibition in human AML decreases EZH2 protein expression and PRC2-based gene regulation. In particular, FLT3 inhibition decreases EZH2 protein stability through non-canonical FLT3 signaling. We modeled the FLT3i-induced myeloid differentiation response seen clinically both in vitro and in vivo using a physiologically relevant murine AML model that expresses *Flt3-ITD* with the loss of *Dnmt3a*. Importantly, complete PRC2 inhibition with the addition of an EZH1/2 inhibitor augments the differentiation effect of FLT3i and significantly reduces leukemic burden. These results demonstrate that FLT3-ITD regulates cell survival and proliferation but also impairs myeloid differentiation in AML, consistent with recent clinical trials using FLT3 inhibitors.

We attempted to elucidate the mechanism by which FLT3 inhibition results in downregulation of EZH2. We showed that FLT3i treatment results in reduced EZH2 protein stability, which is consistent with prior reports.^{29, 30} EZH2 expression showed limited changes with inhibition of AKT or mTORC1 pathways, indicating that the effect of FLT3i is not through these pathways individually. While MEK inhibition led to a moderate reduction in EZH2 expression, the importance of this pathway to FLT3i-induced regulation is unclear given the minimal reduction in protein stability and the known rebound activation of the mitogen-activating protein kinase (MAPK) pathway with >8 hours of FLT3i exposure.⁵² Further studies on the role of MEK are warranted, particularly given the known role of RAS pathway mutations in resistance to FLT3i.^{53–55} Additionally, EZH2 levels were variable across cell lines with CDK1 inhibition despite the consistent alteration in CDK1 phosphorylation upon FLT3 inhibition. These results demonstrate that the mechanisms of signaling by FLT3 remain incompletely described.

We previously showed that FLT3i clinically induces differentiation in *FLT3-ITD* AML patients.^{12, 14} Our results here demonstrating that FLT3-ITD downregulates EZH2 may explain this observation. Here, we were able to model the differentiation effect of FLT3i with murine *Flt3-ITD* AMLs using cooperative mutations common in human *FLT3-ITD* AML and within the bone marrow microenvironment, which has been demonstrated to play a key role in AML survival with FLT3i.^{38, 56–58} The role of EZH2 in myeloid malignancies is complex with tumor suppressive function in leukemia initiation and

oncogenic function in leukemia maintenance.^{19, 59} Our model provides evidence to support an oncogenic role of EZH2 in *FLT3-ITD* AML consistent with prior work in MLL-AF9 and AML1-ETO9a models. Interestingly, treatment of mice with valemestostat alone did not induce myeloid differentiation to a significant degree. The data suggest that FLT3-ITD may suppress myeloid differentiation through kinase-dependent functions other than EZH2 regulation. A recent study confirmed that genetic deletion of *Ezh2* is an incomplete driver of myeloid maturation in *Flt3^{ITD}Npm1^c* leukemia.⁶⁰ Complete understanding of how FLT3-ITD regulates AML differentiation will require further studies.

Our study provides a clear rationale for translating combined FLT3 and PRC2 inhibitors into clinical trials. PRC2 inhibitors must be used cautiously in AML considering its dual role in leukemogenesis and the potential presence of pre-malignant clones in this patient population. Secondary malignancies including myelodysplastic syndrome (MDS) and AML were seen in 2 of 99 follicular lymphoma patients treated with the EZH2 inhibitor, tazemetostat.⁴⁸ Notably, these patients were previously exposed to cytotoxic chemotherapy including anthracyclines and autologous transplant, which on their own have a risk of MDS and AML. Treatment-related MDS and AML have not yet been seen in clinical studies of valemestostat though longer follow-up is needed.⁴⁹ This potential risk may be mitigated in the post-allogeneic transplant population, which may have an added benefit of increased graft-versus-leukemia effect with EZH2 inhibition.⁶¹ We currently cannot predict which patients will respond to FLT3i with differentiation as prior studies did not demonstrate an association with co-mutational status, cytogenetics, or other clinical features.¹⁴ Additional studies are needed to determine which patients may derive the most benefit from enhanced differentiation induced by FLT3 and PRC2 inhibitor combinations. Combinations with RAS targeted therapy may also be beneficial to target clonal outgrowth of RAS mutated monocytic clones.^{54, 55} Overall, however, we propose that differentiation therapy, which has proven remarkably effective for APL, may be feasible and therapeutically advantageous for FLT3-ITD AML.

Supplementary Material

Refer to Web version on PubMed Central for supplementary material.

Acknowledgements:

Shared Resources at Roswell Park Comprehensive Cancer Center were supported by the National Cancer Institute Cancer Center Support Grant 5P30 CA016056 and R50 CA211108. This work was supported by National Institutes of Health grants (R21 CA198621, K08 CA230190, R37 CA226433, and T32 HL007439-36) and the Biff Ruttenberg Foundation. Dr. Sung received additional support from Benjamin and Mary Siddons Measey Foundation, American Society of Hematology, the Leukemia & Lymphoma Society, and the Roswell Park Alliance Foundation. Dr. Carroll receives support from Veterans Administration Merit Award I01BX004662.

Competing interests:

PJS, MS, SSR, HMX, KB, BM, GBW, LP, KK, JP, MJN, BAG, and SS declare no relevant competing interests. RLB has received honoraria from Mission Bio and is a member of the Speakers Bureau for Mission Bio. RLL is on the supervisory board of Qiagen and is a scientific advisor to Imago, Mission Bio, Bakx, Zentalis, Ajax, Auron, Prelude, C4 Therapeutics, and Isoplexis. RLL received research support from Abbvie, constellation, Ajax, Zentalis, and Prelude. RLL has received research support from and consulted for Celgene and Roche and has consulted for Syndax, Incyte, Janssen, Astellas, Morphosys, and Novartis. RLL has received honoraria from Astra Zeneca and Novartis for invited lectures and from Gilead and Novartis for grant reviews. SEM received research funding

from CellCentric. KMB has received research funding from Syndax Pharmaceuticals, Inc. MC is on the Scientific Advisory Board for Cartography Biosciences.

REFERENCES

1. Papaemmanuil E, Gerstung M, Bullinger L, Gaidzik VI, Paschka P, Roberts ND, et al. Genomic Classification and Prognosis in Acute Myeloid Leukemia. *New Engl J Med* 2016; 374(23): 2209 – 2221. [PubMed: 27276561]
2. Mackarehtschian K, Hardin JD, Moore KA, Boast S, Goff SP, Lemischka IR. Targeted disruption of the *flk2/flt3* gene leads to deficiencies in primitive hematopoietic progenitors. *Immunity* 1995; 3(1): 147 – 161. [PubMed: 7621074]
3. Hayakawa F, Towatari M, Kiyoi H, Tanimoto M, Kitamura T, Saito H, et al. Tandem-duplicated *Flt3* constitutively activates *STAT5* and *MAP* kinase and introduces autonomous cell growth in *IL-3*-dependent cell lines. *Oncogene* 2000; 19(5): 624–631. [PubMed: 10698507]
4. Nakao M, Yokota S, Iwai T, Kaneko H, Horiike S, Kashima K, et al. Internal tandem duplication of the *flt3* gene found in acute myeloid leukemia. *Leukemia* 1996; 10(12): 1911 – 1918. [PubMed: 8946930]
5. Kottaridis PD, Gale RE, Frew ME, Harrison G, Langabeer SE, Belton AA, et al. The presence of a *FLT3* internal tandem duplication in patients with acute myeloid leukemia (AML) adds important prognostic information to cytogenetic risk group and response to the first cycle of chemotherapy: analysis of 854 patients from the United Kingdom Medical Research Council AML 10 and 12 trials. *Blood* 2001; 98(6): 1752 – 1759. [PubMed: 11535508]
6. Erba HP, Montesinos P, Kim H-J, Patkowska E, Vrhovac R, Žák P, et al. Quizartinib plus chemotherapy in newly diagnosed patients with *FLT3*-internal-tandem-duplication-positive acute myeloid leukaemia (QuANTUM-First): a randomised, double-blind, placebo-controlled, phase 3 trial. *Lancet* 2023 5/13/2023; 401(10388): 1571–1583. [PubMed: 37116523]
7. Stone RM, Mandrekar SJ, Sanford BL, Laumann K, Geyer S, Bloomfield CD, et al. Midostaurin plus Chemotherapy for Acute Myeloid Leukemia with a *FLT3* Mutation. *New Engl J Med* 2017; 377(5): 454 – 464. [PubMed: 28644114]
8. Cortes JE, Khaled S, Martinelli G, Perl AE, Ganguly S, Russell N, et al. Quizartinib versus salvage chemotherapy in relapsed or refractory *FLT3*-ITD acute myeloid leukaemia (QuANTUM-R): a multicentre, randomised, controlled, open-label, phase 3 trial. *Lancet Oncol* 2019; 20(7): 984–997. [PubMed: 31175001]
9. Perl AE, Martinelli G, Cortes JE, Neubauer A, Berman E, Paolini S, et al. Gilteritinib or Chemotherapy for Relapsed or Refractory *FLT3*-Mutated AML. *New Engl J Med* 2019; 381(18): 1728 – 1740. [PubMed: 31665578]
10. Kiyoi H, Ohno R, Ueda R, Saito H, Naoe T. Mechanism of constitutive activation of *FLT3* with internal tandem duplication in the juxtamembrane domain. *Oncogene* 2002; 21(16): 2555–2563. [PubMed: 11971190]
11. Levis M, Allebach J, Tse K-F, Zheng R, Baldwin BR, Smith BD, et al. A *FLT3*-targeted tyrosine kinase inhibitor is cytotoxic to leukemia cells in vitro and in vivo. *Blood* 2002; 99(11): 3885–3891. [PubMed: 12010785]
12. Nybakken GE, Canaani J, Roy D, Morrissette JD, Watt CD, Shah NP, et al. Quizartinib elicits differential responses that correlate with karyotype and genotype of the leukemic clone. *Leukemia* 2015; 30(6): 1422 – 1425. [PubMed: 26585411]
13. Sexauer A, Perl A, Yang X, Borowitz M, Gocke C, Rajkhowa T, et al. Terminal myeloid differentiation in vivo is induced by *FLT3* inhibition in *FLT3*/ITD AML. *Blood* 2012; 120(20): 4205 – 4214. [PubMed: 23012328]
14. McMahon CM, Canaani J, Rea B, Sargent RL, Qualtieri JN, Watt CD, et al. Gilteritinib induces differentiation in relapsed and refractory *FLT3*-mutated acute myeloid leukemia. *Blood Adv* 2019; 3(10): 1581 – 1585. [PubMed: 31122910]
15. Levis MJ, Perl AE, Altman JK, Gocke CD, Bahceci E, Hill J, et al. A next-generation sequencing-based assay for minimal residual disease assessment in AML patients with *FLT3*-ITD mutations. *Blood Adv* 2018; 2(8): 825 – 831. [PubMed: 29643105]

16. Lo-Coco F, Avvisati G, Vignetti M, Thiede C, Orlando SM, Iacobelli S, et al. Retinoic acid and arsenic trioxide for acute promyelocytic leukemia. *New Engl J Med* 2013; 369(2):111 – 121. [PubMed: 23841729]
17. Pv Galen, Hovestadt V, Ii MHW, Hughes TK, Griffin GK, Battaglia S, et al. Single-Cell RNA-Seq Reveals AML Hierarchies Relevant to Disease Progression and Immunity. *Cell* 2019; 176(6): 1265–1281.e1224. [PubMed: 30827681]
18. Margueron R, Reinberg D. The Polycomb complex PRC2 and its mark in life. *Nature* 2011; 469(7330): 343 – 349. [PubMed: 21248841]
19. Basheer F, Giotopoulos G, Meduri E, Yun H, Mazan M, Sasca D, et al. Contrasting requirements during disease evolution identify EZH2 as a therapeutic target in AML. *J Exp Med* 2019; 216(4): 966 –981. [PubMed: 30890554]
20. Neff T, Sinha AU, Kluk MJ, Zhu N, Khattab MH, Stein L, et al. Polycomb repressive complex 2 is required for MLL-AF9 leukemia. *Proc Nat Acad Sci USA* 2012; 109(13): 5028 – 5033. [PubMed: 22396593]
21. Tanaka S, Miyagi S, Sashida G, Chiba T, Yuan J, Mochizuki-Kashio M, et al. Ezh2 augments leukemogenicity by reinforcing differentiation blockage in acute myeloid leukemia. *Blood* 2012; 120(5): 1107 – 1117. [PubMed: 22677129]
22. Xu B, On DM, Ma A, Parton T, Konze KD, Pattenden SG, et al. Selective inhibition of EZH2 and EZH1 enzymatic activity by a small molecule suppresses MLL-rearranged leukemia. *Blood* 2015; 125(2): 346 – 357. [PubMed: 25395428]
23. Meyer SE, Qin T, Muench DE, Masuda K, Venkatasubramanian M, Orr E, et al. DNMT3A Haploinsufficiency Transforms FLT3ITD Myeloproliferative Disease into a Rapid, Spontaneous, and Fully Penetrant Acute Myeloid Leukemia. *Cancer Discovery* 2016; 6(5): 501 – 515. [PubMed: 27016502]
24. Colligan SH, Amitrano AM, Zollo RA, Peresie J, Kramer ED, Morreale B, et al. Inhibiting the biogenesis of myeloid-derived suppressor cells enhances immunotherapy efficacy against mammary tumor progression. *J Clin Investigation* 2022; 132(23): e158661.
25. DiNardo CD, Stein EM, Botton Sd, Roboz GJ, Altman JK, Mims AS, et al. Durable Remissions with Ivosidenib in IDH1-Mutated Relapsed or Refractory AML. *New Engl J Med* 2018; 378(25): 2386–2398. [PubMed: 29860938]
26. Erba HP, Fathi AT, Issa GC, Altman JK, Montesinos P, Patnaik MM, et al. Update on a Phase 1/2 First-in-Human Study of the Menin-KMT2A (MLL) Inhibitor Ziftomenib (KO-539) in Patients with Relapsed or Refractory Acute Myeloid Leukemia. *Blood* 2022; 140(Supplement 1): 153–156.
27. Issa GC, Aldoss I, DiPersio JF, Cuglievan B, Stone RM, Arellano ML, et al. The Menin Inhibitor SNDX-5613 (revumenib) Leads to Durable Responses in Patients (Pts) with KMT2A -Rearranged or NPM1 Mutant AML: Updated Results of a Phase (Ph) 1 Study. *Blood* 2022; 140(Supplement 1): 150–152.
28. Stein EM, DiNardo CD, Pollyea DA, Fathi AT, Roboz GJ, Altman JK, et al. Enasidenib in mutant IDH2 relapsed or refractory acute myeloid leukemia. *Blood* 2017; 130(6): 722–731. [PubMed: 28588020]
29. Wei Y, Chen Y-H, Li L-Y, Lang J, Yeh S-P, Shi B, et al. CDK1-dependent phosphorylation of EZH2 suppresses methylation of H3K27 and promotes osteogenic differentiation of human mesenchymal stem cells. *Nat Cell Biol* 2010; 13(1): 87 – 94. [PubMed: 21131960]
30. Göllner S, Oellerich T, Agrawal-Singh S, Schenk T, Klein H-U, Rohde C, et al. Loss of the histone methyltransferase EZH2 induces resistance to multiple drugs in acute myeloid leukemia. *Nat Med* 2017; 23(1): 69 – 78. [PubMed: 27941792]
31. James AJ, Smith CC, Litzow M, Perl AE, Altman JK, Shepard D, et al. Pharmacokinetic Profile of Gilteritinib: A Novel FLT-3 Tyrosine Kinase Inhibitor. *Clin Pharmacokinet* 2020; 59(10): 1273–1290. [PubMed: 32304015]
32. Cerami E, Gao J, Dogrusoz U, Gross BE, Sumer SO, Aksoy BA, et al. The cBio Cancer Genomics Portal: An Open Platform for Exploring Multidimensional Cancer Genomics Data. *Cancer Discovery* 2012; 2(5): 401–404. [PubMed: 22588877]

33. Lindsley RC, Mar BG, Mazzola E, Grauman PV, Shareef S, Allen SL, et al. Acute myeloid leukemia ontogeny is defined by distinct somatic mutations. *Blood* 2015; 125(9): 1367–1376. [PubMed: 25550361]
34. The Cancer Genome Atlas Network. Genomic and epigenomic landscapes of adult de novo acute myeloid leukemia. *New Engl J Med* 2013; 368(22): 2059 – 2074. [PubMed: 23634996]
35. Tyner JW, Tognon CE, Bottomly D, Wilmot B, Kurtz SE, Savage SL, et al. Functional genomic landscape of acute myeloid leukaemia. *Nature* 2018; 562(7728): 526 – 531. [PubMed: 30333627]
36. Fujii S, Fukamachi K, Tsuda H, Ito K, Ito Y, Ochiai A. RAS oncogenic signal upregulates EZH2 in pancreatic cancer. *Biochem Bioph Res Co* 2012; 417(3): 1074–1079.
37. Riquelme E, Behrens C, Lin HY, Simon G, Papadimitrakopoulou V, Izzo J, et al. Modulation of EZH2 Expression by MEK-ERK or PI3K-AKT Signaling in Lung Cancer Is Dictated by Different KRAS Oncogene Mutations. *Cancer Res* 2016; 76(3): 675–685. [PubMed: 26676756]
38. Sung PJ, Sugita M, Koblish H, Perl AE, Carroll M. Hematopoietic cytokines mediate resistance to targeted therapy in FLT3-ITD acute myeloid leukemia. *Blood Adv* 2019; 3(7): 1061 – 1072. [PubMed: 30944098]
39. Kim J, Woo AJ, Chu J, Snow JW, Fujiwara Y, Kim CG, et al. A Myc Network Accounts for Similarities between Embryonic Stem and Cancer Cell Transcription Programs. *Cell* 2010; 143(2): 313–324. [PubMed: 20946988]
40. Melgar K, Walker MM, Jones LM, Bolanos LC, Hueneman K, Wunderlich M, et al. Overcoming adaptive therapy resistance in AML by targeting immune response pathways. *Science translational medicine* 2019; 11(508): eaaw8828. [PubMed: 31484791]
41. Park HJ, Gregory MA, Zaberezhnyy V, Goodspeed A, Jordan CT, Kieft JS, et al. Therapeutic resistance in acute myeloid leukemia cells is mediated by a novel ATM/mTOR pathway regulating oxidative phosphorylation. *Elite* 2022; 11: e79940.
42. Lenard A, Xie HM, Pastuer T, Shank T, Libbrecht C, Kingsley M, et al. Epigenetic regulation of protein translation in KMT2A-rearranged AML. *Exp Hematol* 2020; 85: 57–69. [PubMed: 32437908]
43. Park DJ, Vuong PT, Vos Sd, Douer D, Koeffler HP. Comparative analysis of genes regulated by PML/RAR α and PLZF/RAR α in response to retinoic acid using oligonucleotide arrays. *Blood* 2003; 102(10): 3727–3736. [PubMed: 12893766]
44. Zheng R, Friedman AD, Levis M, Li L, Weir EG, Small D. Internal tandem duplication mutation of FLT3 blocks myeloid differentiation through suppression of C/EBP α expression. *Blood* 2004; 103(5): 1883 – 1890. [PubMed: 14592841]
45. Lavau C, Szilvassy SJ, Slany R, Cleary ML. Immortalization and leukemic transformation of a myelomonocytic precursor by retrovirally transduced HRX-ENL. *Embo J* 1997; 16(14): 4226–4237. [PubMed: 9250666]
46. Radomska HS, Bassères DS, Zheng R, Zhang P, Dayaram T, Yamamoto Y, et al. Block of C/EBP α function by phosphorylation in acute myeloid leukemia with FLT3 activating mutations. *Journal of Experimental Medicine* 2006; 203(2): 371–381. [PubMed: 16446383]
47. Bowman RL, Dunbar A, Mishra T, Xiao W, Waarts MR, Maestre IF, et al. Modeling clonal evolution and oncogenic dependency in vivo in the context of hematopoietic transformation. *Biorxiv* 2022: 2022.2005.2018.492524.
48. Morschhauser F, Tilly H, Chaidos A, McKay P, Phillips T, Assouline S, et al. Tazemetostat for patients with relapsed or refractory follicular lymphoma: an open-label, single-arm, multicentre, phase 2 trial. *Lancet Oncol* 2020; 21(11): 1433–1442. [PubMed: 33035457]
49. Izutsu K, Makita S, Nosaka K, Yoshimitsu M, Utsunomiya A, Kusumoto S, et al. An Open-Label, Single-Arm, Phase 2 Trial of Valemetostat in Relapsed or Refractory Adult T-Cell Leukemia/ Lymphoma. *Blood* 2023; 141(10): 1159–1168. [PubMed: 36150143]
50. Fujita S, Honma D, Adachi N, Araki K, Takamatsu E, Katsumoto T, et al. Dual inhibition of EZH1/2 breaks the quiescence of leukemia stem cells in acute myeloid leukemia. *Leukemia* 2018; 32(4): 855 – 864. [PubMed: 28951561]
51. Pronk CJH, Rossi DJ, Månsson R, Attema JL, Norddahl GL, Chan CKF, et al. Elucidation of the Phenotypic, Functional, and Molecular Topography of a Myeloerythroid Progenitor Cell Hierarchy. *Cell Stem Cell* 2007; 1(4): 428–442. [PubMed: 18371379]

52. Bruner JK, Ma HS, Li L, Qin ACR, Rudek MA, Jones RJ, et al. Adaptation to TKI Treatment Reactivates ERK Signaling in Tyrosine Kinase-Driven Leukemias and Other Malignancies. *Cancer Res* 2017; 77(20): 5554 – 5563. [PubMed: 28923853]
53. Joshi SK, Nechiporuk T, Bottomly D, Piehowski PD, Reisz JA, Pittsenbarger J, et al. The AML microenvironment catalyzes a stepwise evolution to gilteritinib resistance. *Cancer Cell* 2021; 39(7): 999–1014.e1018. [PubMed: 34171263]
54. Kennedy VE, Peretz C, Lee P, Chyla B, Sun Y, Dail M, et al. Multi-Omic Single-Cell Sequencing Reveals Genetic and Immunophenotypic Clonal Selection in Patients With FLT3-Mutated AML Treated With Gilteritinib/Venetoclax. *Blood* 2022; 140(Supplement 1): 2244–2246.
55. McMahon CM, Ferng T, Canaani J, Wang ES, Morrissette JJD, Eastburn DJ, et al. Clonal Selection with RAS Pathway Activation Mediates Secondary Clinical Resistance to Selective FLT3 Inhibition in Acute Myeloid Leukemia. *Cancer Discovery* 2019; 9(8): 1050–1063. [PubMed: 31088841]
56. Buelow DR, Bhatnagar B, Orwick S, Jeon JY, Eisenmann ED, Stromatt JC, et al. BMX Kinase Mediates Gilteritinib Resistance in FLT3-mutated AML through Microenvironmental Factors. *Blood Advances* 2022; 6(17): 5049–5060. [PubMed: 35797240]
57. Traer E, Martinez J, Javidi-Sharifi N, Agarwal A, Dunlap J, English I, et al. FGF2 from Marrow Microenvironment Promotes Resistance to FLT3 Inhibitors in Acute Myeloid Leukemia. *Cancer Res* 2016; 76(22): 6471 – 6482. [PubMed: 27671675]
58. Yang X, Sexauer A, Levis M. Bone marrow stroma-mediated resistance to FLT3 inhibitors in FLT3-ITD AML is mediated by persistent activation of extracellular regulated kinase. *Brit J Haematol* 2014; 164: 61 – 72. [PubMed: 24116827]
59. Sashida G, Harada H, Matsui H, Oshima M, Yui M, Harada Y, et al. Ezh2 loss promotes development of myelodysplastic syndrome but attenuates its predisposition to leukaemic transformation. *Nature communications* 2014; 5(1): 4177.
60. Lara-Astiaso D, Goñi-Salaverri A, Mendieta-Esteban J, Narayan N, Del Valle C, Gross T, et al. In vivo screening characterizes chromatin factor functions during normal and malignant hematopoiesis. *Nature Genetics* 2023; 55(9): 1542–1554. [PubMed: 37580596]
61. Gambacorta V, Beretta S, Ciccimarra M, Zito L, Giannetti K, Andrisani A, et al. Integrated Multiomic Profiling Identifies the Epigenetic Regulator PRC2 as a Therapeutic Target to Counteract Leukemia Immune Escape and Relapse. *Cancer Discovery* 2022; 12(6): 1449–1461. [PubMed: 35255120]

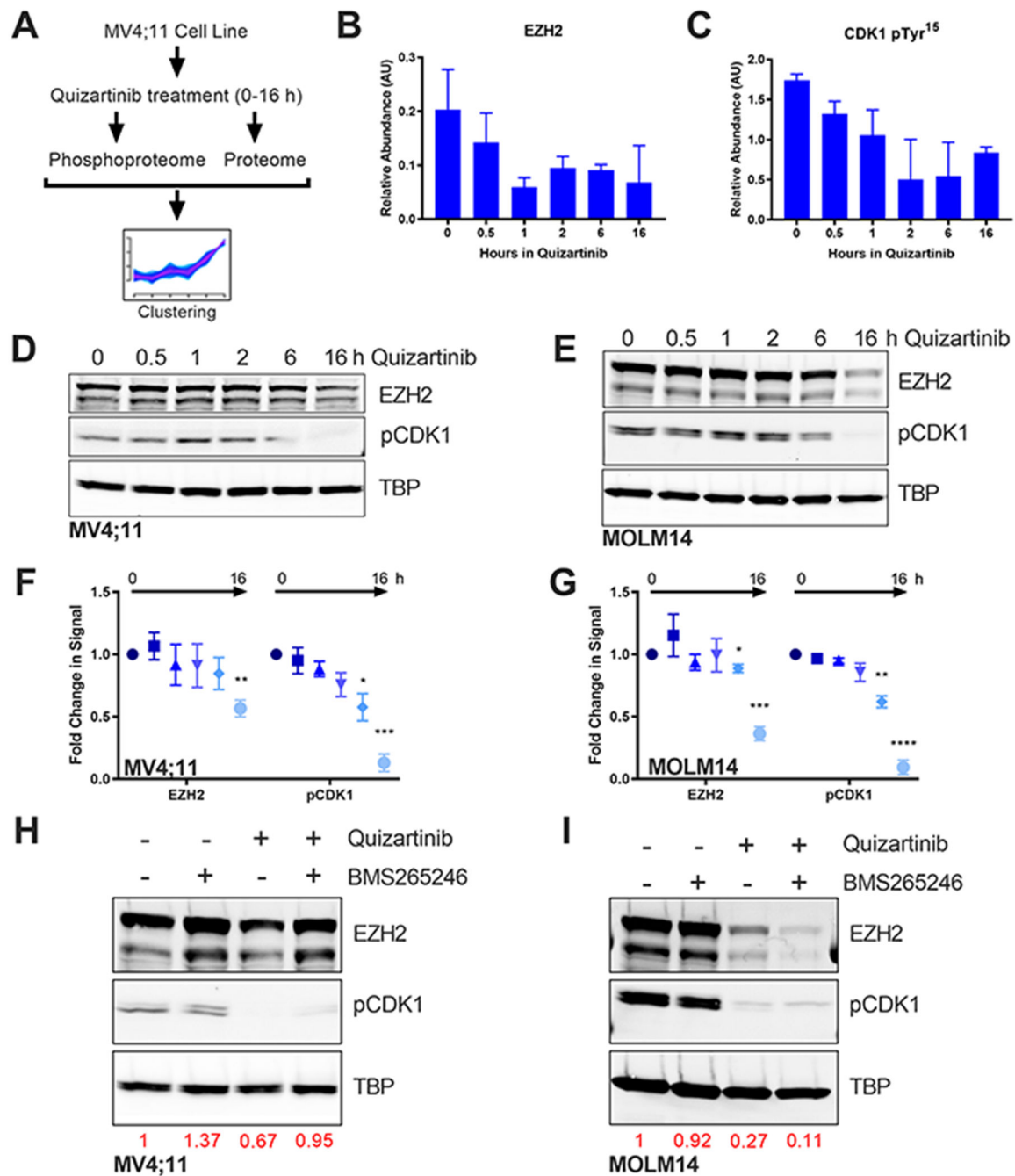


Fig. 1. EZH2 is downregulated by FLT3 inhibition in AML cell lines.

(A) Schematic of proteomic based screen. (B,C) Relative abundance of (B) EZH2 and (C) CDK1 phosphotyrosine 15 peptides for 0-16 hours of treatment with 20 nM quizartinib. Bars represent mean \pm standard deviation (n = 2). (D,E) Immunoblot for EZH2 and phospho-CDK1 Y15 in (D) MV4;11 and (E) MOLM14 cells for 0-16 hours of treatment with quizartinib. (F,G) Quantification of EZH2 and pCDK1 expression for (F) MV4;11 and (G) MOLM14 normalized to TBP loading control. (H,I) Immunoblot for EZH2 and phospho-CDK1 Y15 in (H) MV4;11 and (I) MOLM14 cells treated with DMSO or 100 nM

CDK1 inhibitor (BMS265246) for 16 hours followed by treatment with 24 hours DMSO or 20 nM quizartinib. Fold change in normalized EZH2 denoted in red.

Author Manuscript

Author Manuscript

Author Manuscript

Author Manuscript

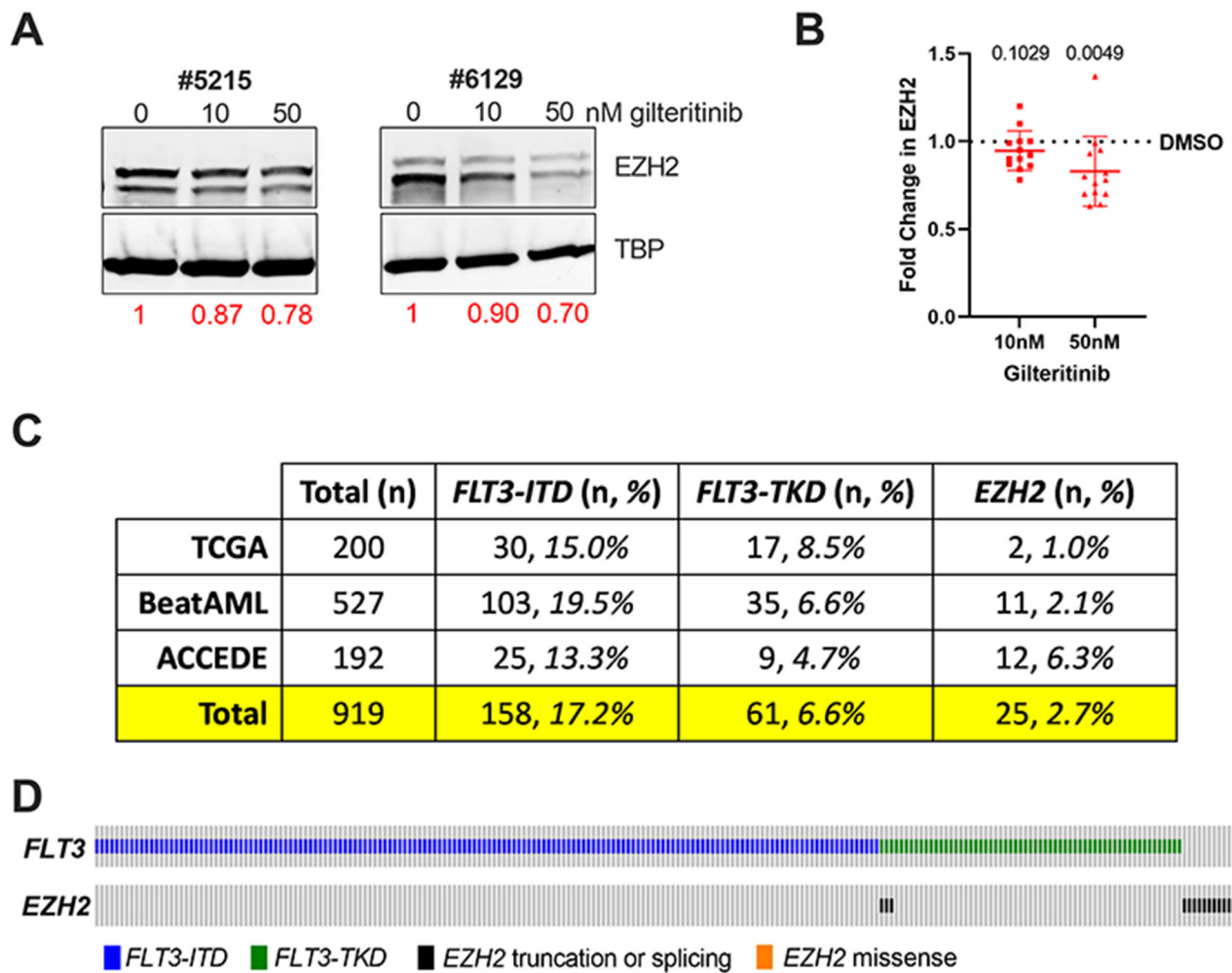


Fig. 2. EZH2 is downregulated by FLT3 inhibition in primary AML.

(A) Representative immunoblots for EZH2 in patient AML mononuclear cells treated with indicated dose of gilteritinib for 24 hours. Quantification of EZH2 normalized to TBP and represented as fold change from the 0 nM (DMSO) condition in red. (B) Summary of EZH2 quantification from 13 primary AML specimens treated as in (A). Data is normalized to DMSO control for each sample, represented as a dashed line. Each dot is an individual patient. Solid line represents mean \pm SEM (n = 13) with p-value from two-sided t-test. (C) Summary of *FLT3* and *EZH2* mutational status of patients from TCGA, BeatAML, and ACCEDE datasets [ref. 33–35]. (D) Oncoprint of *FLT3* and *EZH2* mutational status for individual patients. Additional patients lacking either mutation are not depicted.

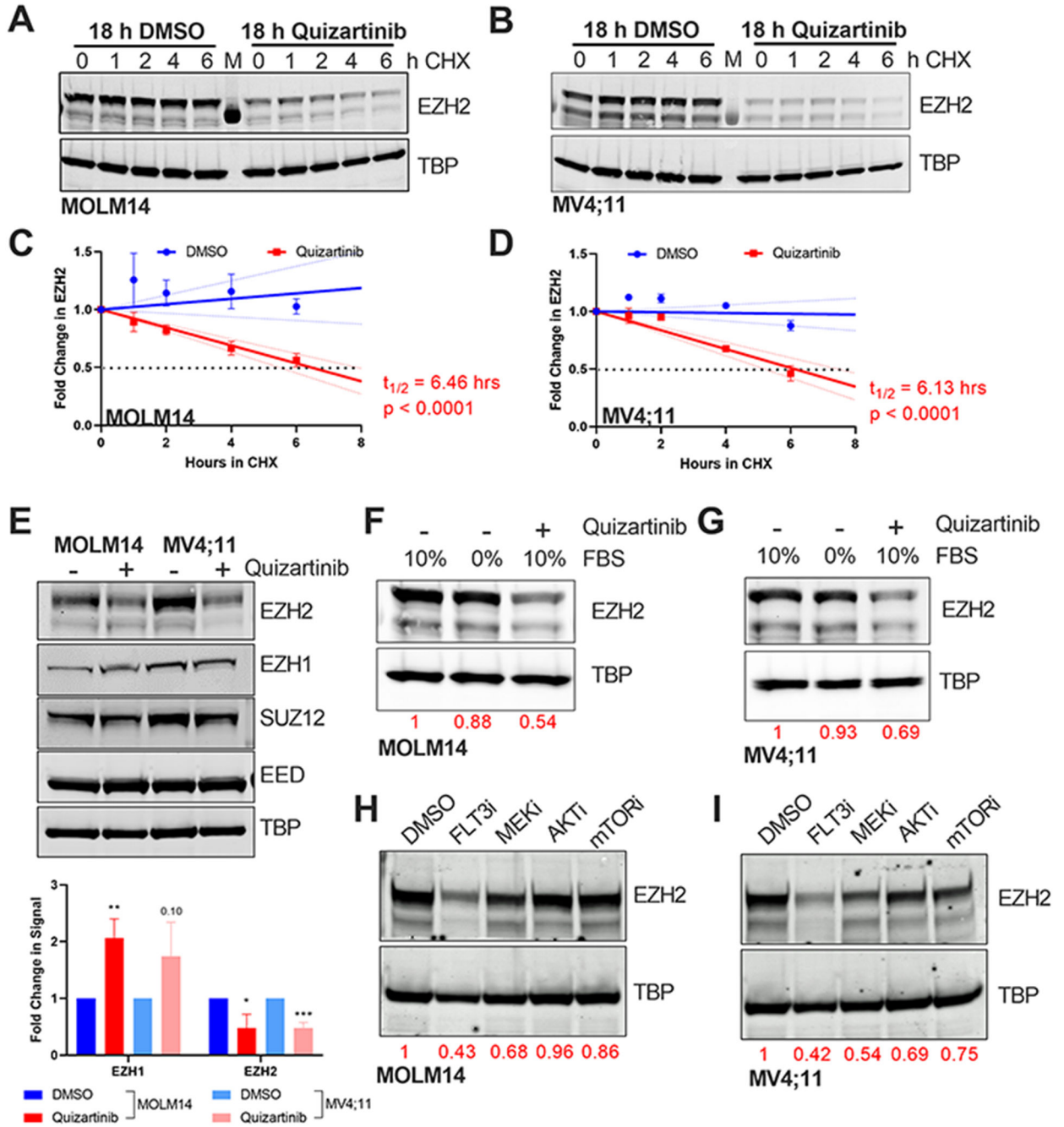


Fig. 3. FLT3i induce EZH2 protein instability.

(A,B) Immunoblot for EZH2 in (A) MOLM14 and (B) MV4;11 cells treated with DMSO or quizartinib for 18 hours followed by 0-6 hours of cycloheximide (CHX). (C,D) Quantification of EZH2 expression for (C) MOLM14 and (D) MV4;11 normalized to TBP loading control and represented as mean fold change from the 0 hour CHX condition for each drug treatment \pm SEM (n = 3). Solid lines represent simple linear regression models, which were used to calculate the half-life of EZH2. Dashed lines represent 95% confidence intervals. P-values are for non-zero slope of regression. (E) Immunoblot for

PRC2 components in MOLM14 and MV4;11 cells treated with quizartinib for 16 hours. Quantification of mean fold change in normalized EZH1 and EZH2 expression in bar graph below. Error bars represent SEM (n=3). **(F,G)** Immunoblot of EZH2 in **(F)** MOLM14 and **(G)** MV4;11 cells in 10% or 0% serum and treated with DMSO or quizartinib for 16 hours. **(H,I)** Immunoblot of EZH2 in **(H)** MOLM14 and **(I)** MV4;11 cells treated with DMSO, quizartinib, 10 nM trametinib (MEKi), 1 μ M capivasertib (AKTi), or 100 nM rapamycin (mTORi) for 20 hours. Fold change in normalized EZH2 denoted in red.

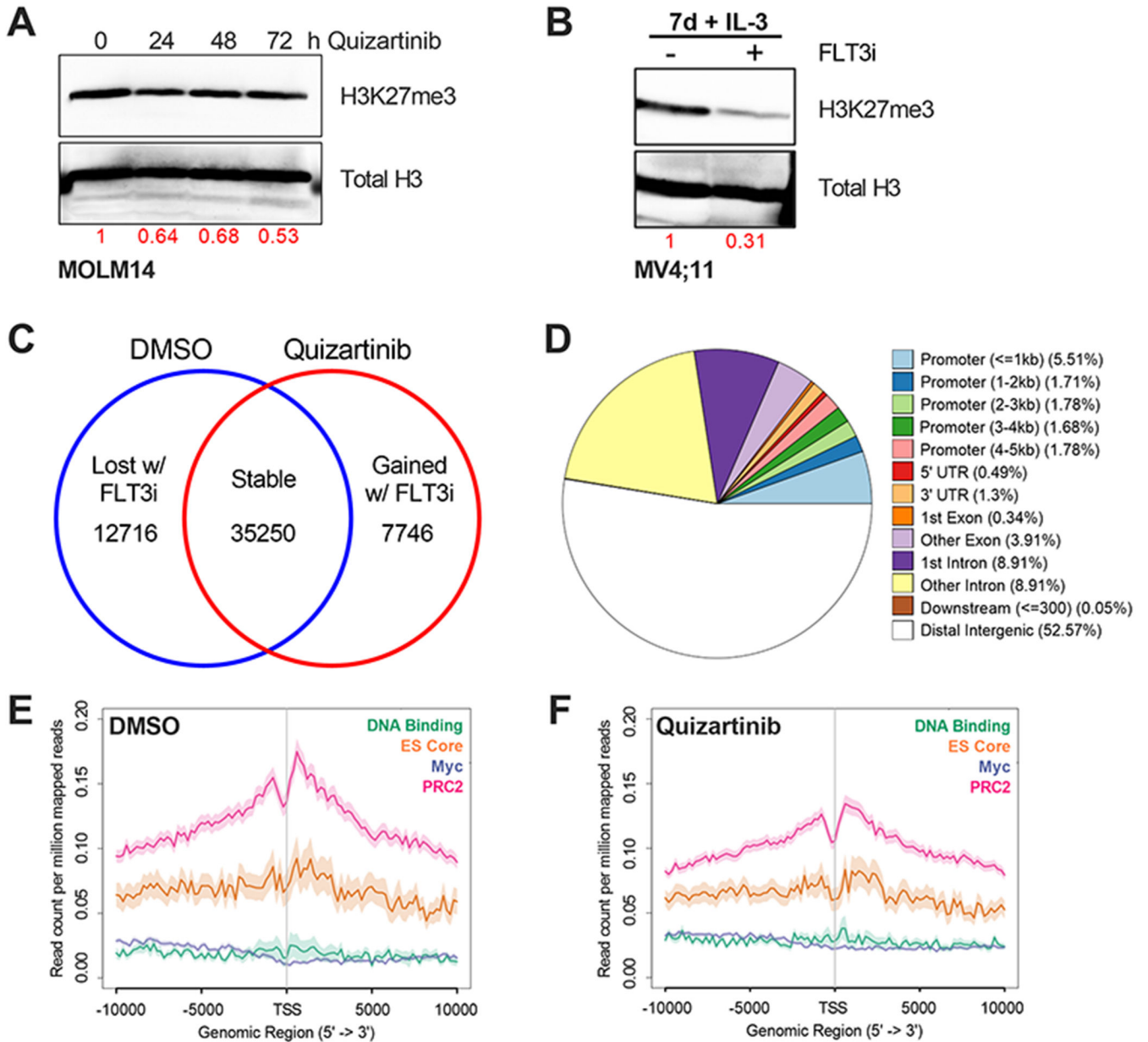


Fig. 4. FLT3i reduce H3K27me3 at PRC2 target genes.

(A) Immunoblot for H3K27me3 and total H3 of histone extracts from MOLM14 cells treated for 0-72 hours with quizartinib. Fold change in normalized H3K27me3 denoted in red. (B) Immunoblot for H3K27me3 and total H3 of histone extracts from MV4;11 cells treated with DMSO or 20 nM crenolanib for 7 days. Both samples were cultured with 20 ng/ml IL-3. Fold change in normalized H3K27me3 denoted in red. (C) Number of H3K27me3 ChIP-seq peaks from MOLM14 cells treated with DMSO or quizartinib for 24 hours. (D) Summary of peak distribution across all samples. (E,F) H3K27me3 ChIP-Seq read count across the gene body for PRC2, Myc, ES Core, and DNA Binding target gene sets defined in Neff et al. [ref. 20] for (E) DMSO and (F) quizartinib.

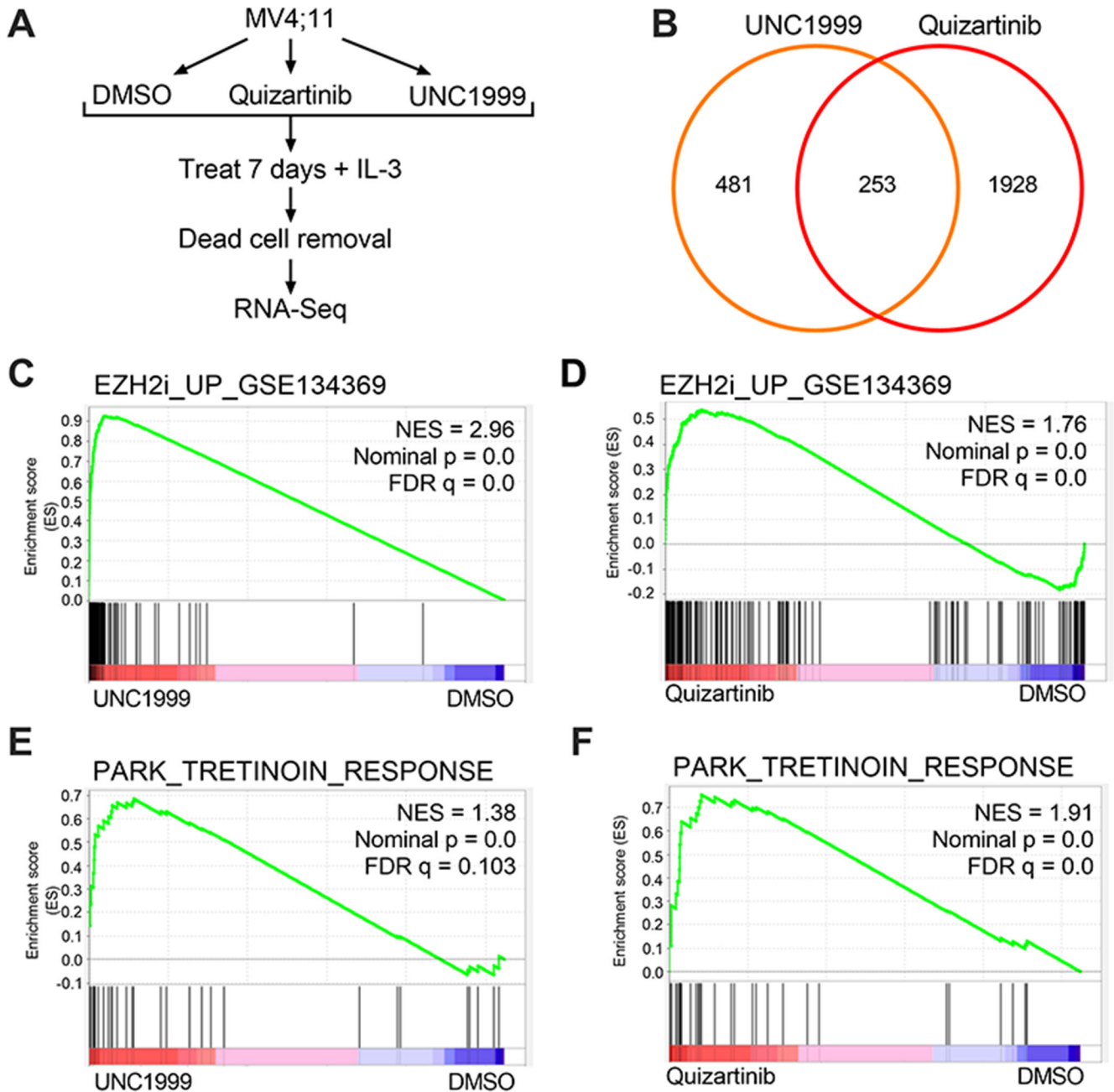


Fig. 5. FLT3i increase expression of PRC2 target genes.

(A) Schematic of sample preparation for RNA-Seq from MV4;11 cells treated with IL-3 plus DMSO, quizartinib or 1 μ M UNC1999. (B) Number of differentially expressed genes from RNA-Seq analysis (cut off log₂ fold change >1 or <-1, adjusted p < 0.05). Overlapping genes includes only those with same directionality of change. (C,D) GSEA of (C) UNC1999 or (D) quizartinib treated samples with GSK126 upregulated genes from Lenard et al. [ref. 42]. (E,F) GSEA of (E) UNC1999 or (F) quizartinib treated samples with tretinoin responsive genes from Park et al. [ref. 43].

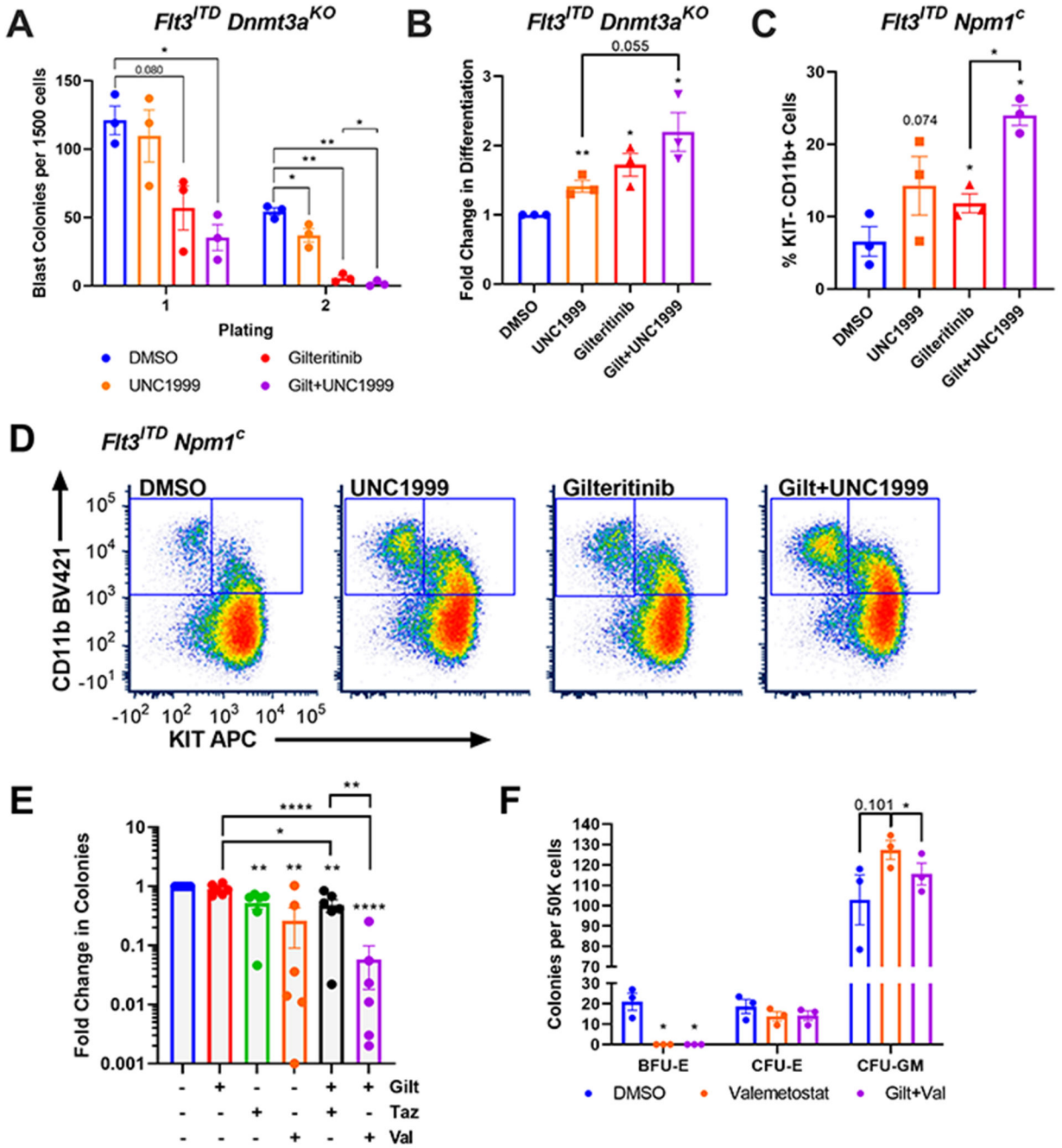


Fig. 6. FLT3i and PRC2i promote myeloid differentiation in murine and human AML.

(A) Number of blast colonies over two platings from KIT⁺ splenocytes from different primary *FIt3^{ITD} Dnmt3a^{KO}* AML mice. Cells were treated with DMSO, 1 μ M UNC1999, 50 nM gilteritinib, or the combination. Each dot is an individual murine AML sample. Bars represent mean \pm SEM (n = 3). (B) Fold change in percentage of differentiated colonies enumerated from the first plating in (A). Bars represent mean \pm SEM (n = 3). (C) Percentage of KIT- CD11b⁺ *FIt3^{ITD} Npm1^C* AML cells treated for 4-5 days with indicated drugs. Bars represent mean \pm SEM (n = 3). (D) Flow plots of CD11b and KIT expression of cells in (C).

(E) Colony forming activity of six primary human AML BM MNCs (samples CI-00299642, CI-00301459, and 16-0760) treated with DMSO, 50 nM gilteritinib, 1 μ M tazemetostat, 100 nM valemetostat, gilteritinib + tazemetostat, or gilteritinib + valemetostat. Note that Y-axis is in log scale. All samples were counted in technical duplicates. Each dot is an individual patient sample. Bars represent mean \pm SEM (n = 6). (F) Colony forming activity of normal human BM MNCs treated with DMSO, valemetostat, or gilteritinib + valemetostat. Bars represent mean \pm SEM (n = 3).

Author Manuscript

Author Manuscript

Author Manuscript

Author Manuscript

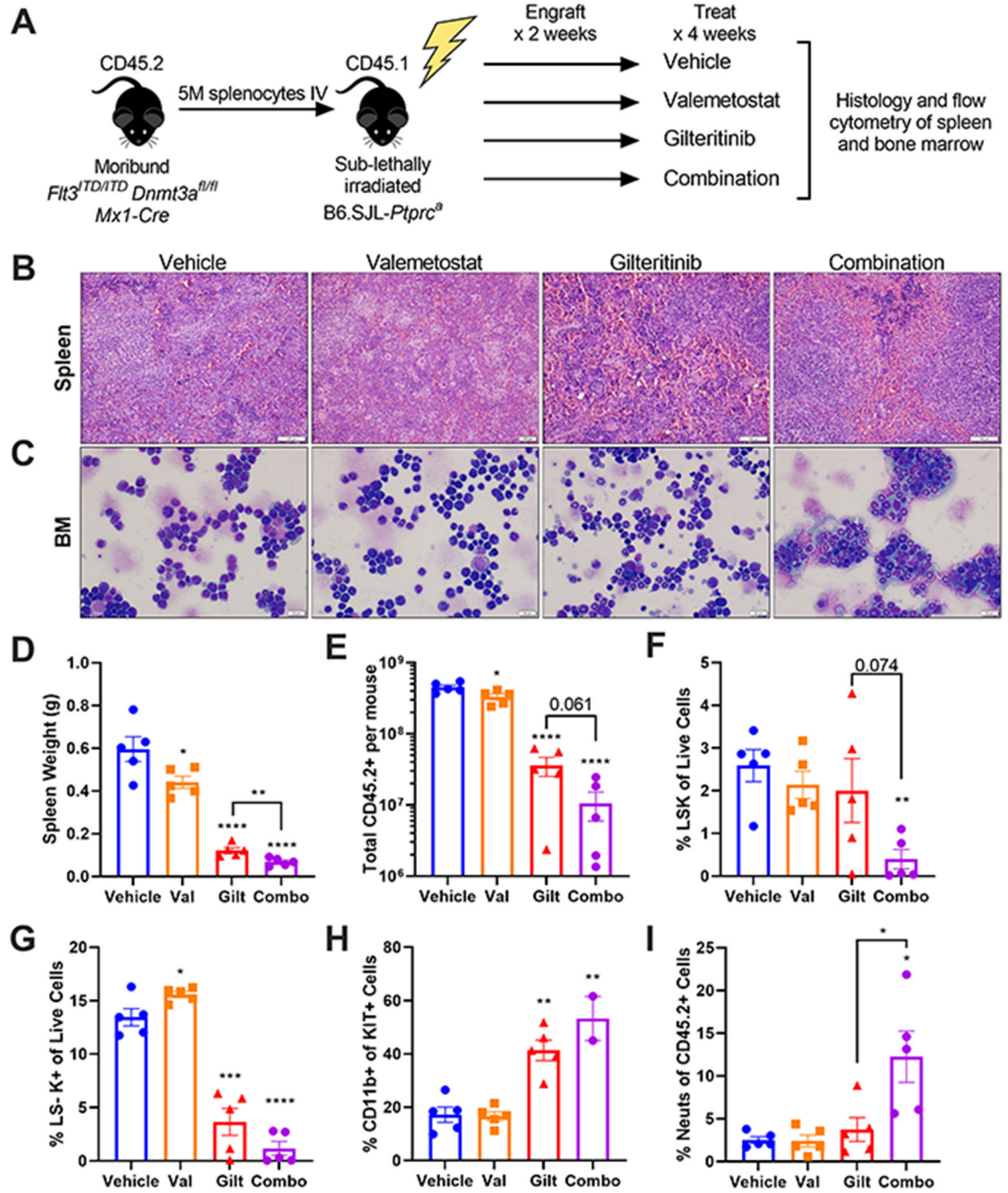


Figure 7. FLT3i and PRC2i reduce leukemic burden and promote differentiation in vivo.

(A) Schematic of secondary transplantation model. (B) Representative images of H&E-stained spleen sections. (C) Representative images of Wright-Giemsa-stained bone marrow aspirates. Bar graphs of (D) spleen weights, (E) total CD45.2+ cells per mouse, (F) percent Lin- Sca1+ Kit+ of live cells in spleen, (G) percent Lin- Sca1- Kit+ of live cells in spleen, (H) percent CD11b+ of Kit+ cells in spleen, and (I) percent neutrophils of CD45.2+ cells

in spleen. Each dot is an individual mouse. Bars represent mean \pm SEM ($n = 5$). Samples omitted in (H) with fewer than 1000 Kit+ cells analyzed for some combination treated mice.

Author Manuscript

Author Manuscript

Author Manuscript

Author Manuscript